

The smaller impact parameters have small values of  $dV/dr$  for the smaller radial distances, whereas the larger impact parameters have a larger and nearly constant value of  $dV/dr$ . These very different driving forces may contribute to the sharpness of the angular distribution. The variation of the mass distribution and the average TKE with angle of detection of the light fragment can also be qualitatively explained. Small values of  $dV/dr$  at small  $r$  for systems of small impact parameter allow deeper penetration and longer lifetimes for mass transfer. As seen in Fig. 3(b), the mass exchange between target and projectile at  $59^\circ$  (lab) is considerably greater than observed at  $34^\circ$  (lab). Also, the average TKE has its lowest measured value at  $59^\circ$  (lab), consistent with smaller values of angular momentum relative to more forward angles and a correspondingly lower value of the rotational energy to be added to the Coulomb energy to give the ob-

served TKE.

\*Work performed under the auspices of the U. S. Atomic Energy Commission.

†John Simon Guggenheim Fellow, Niels Bohr Institute, Copenhagen, Denmark.

‡Permanent address: Fachbereich Physik, Universität Marburg, Marburg, Germany.

<sup>1</sup>A. G. Artukh, G. F. Gridnev, V. L. Mikheev, V. V. Volkov, and J. Wilczynski, Nucl. Phys. **A215**, 91 (1973).

<sup>2</sup>F. Hanappe, M. Lefort, C. Ngo, J. Peter, and B. Tamain, Phys. Rev. Lett. **32**, 738 (1974).

<sup>3</sup>R. Vandenbosch and J. R. Huizenga, *Nuclear Fission* (Academic, New York, 1973), see references to Chap. 6.

<sup>4</sup>J. Wilczynski, Phys. Lett. **47B**, 484 (1973).

<sup>5</sup>J. S. Blair, Phys. Rev. **95**, 1218 (1954); W. E. Frahn, Ann. Phys. (New York) **72**, 524 (1972).

<sup>6</sup>J. Wilczynski, Nucl. Phys. **A216**, 386 (1973).

<sup>7</sup>J. R. Huizenga, U. S. Atomic Energy Commission Progress Report No. COO-3496-44, 1974 (unpublished).

## Observations of a High-Spin Yrast Cascade in $^{50}\text{Cr}$

W. Kutschera, R. B. Huber, C. Signorini,\* and H. Morinaga

*Physik Department der Technischen Universität München, 8046 Garching, Germany*

(Received 10 July 1974)

A ground-state band with spin up to  $J^\pi = 12^+$  was observed in  $^{50}\text{Cr}$  from the reactions  $^{40}\text{Ca}(^{16}\text{O}, 2p\alpha)^{50}\text{Cr}$ ,  $^{24}\text{Mg}(^{32}\text{S}, 2p\alpha)^{50}\text{Cr}$ ,  $^{40}\text{Ca}(^{14}\text{N}, 3pn)^{50}\text{Cr}$ , and  $^{40}\text{Ca}(^{12}\text{C}, 2p)^{50}\text{Cr}$ . Spin and parity assignments were made from  $\gamma$ - $\gamma$  coincidences, angular distributions, and linear-polarization measurements. The higher-spin states are reasonably well reproduced in the  $(1f_{7/2})^n$  shell-model frame while discrepancies exist for the lower ones. These levels have collective features at lower excitation but very pure shell-model characteristics towards the maximum spin expected in the  $(1f_{7/2})^n$  space.

During a systematic  $\gamma$ -ray study<sup>1-3</sup> of high-spin states in  $1f_{7/2}$  nuclei, a strong selective excitation of the ground-state band of  $^{50}\text{Cr}$  was observed with various heavy-ion compound reactions:  $^{40}\text{Ca}(^{16}\text{O}, 2p\alpha)^{50}\text{Cr}$ ,  $^{24}\text{Mg}(^{32}\text{S}, 2p\alpha)^{50}\text{Cr}$ ,  $^{40}\text{Ca}(^{14}\text{N}, 3pn)^{50}\text{Cr}$ , and  $^{40}\text{Ca}(^{12}\text{C}, 2p)^{50}\text{Cr}$ . In each of these reactions the ground-state-band cascade was found to continue above the known  $6^+$  state<sup>4</sup> with four additional strong transitions connecting states with presumably high spin. The coincidence spectra for the reaction  $^{40}\text{Ca}(^{16}\text{O}, 2p\alpha)^{50}\text{Cr}$  are shown in Fig. 1.

The nucleus  $^{50}\text{Cr}$  is particularly interesting because its low-energy level structure shows<sup>4</sup> rather high collectivity. Recent measurements<sup>5</sup> of the static quadrupole moment of the lowest  $2^+$  state suggest a large prolate ground-state defor-

mation. However, the decrease of the  $B(E2)$  values of the ground-state band with increasing spin<sup>4</sup> indicates a decrease of the collectivity for the higher-spin states. Thus, it is interesting to see how the ground-state band behaves at the higher-spin side, especially concerning the collectivity. In fact, the states with highest spin until now reported in the  $1f_{7/2}$  shell, namely, the  $J^\pi = \frac{19}{2}^-$  states in  $^{43}\text{Sc}$ <sup>6</sup> and  $^{53}\text{Fe}$ ,<sup>7</sup> are well described by the pure  $(1f_{7/2})^n$  configuration. In the same space, spins up to  $14^+$  are expected for  $^{50}\text{Cr}$ .

In order to investigate the new high-spin levels found in  $^{50}\text{Cr}$  the reaction  $^{40}\text{Ca}(^{16}\text{O}, 2p\alpha)^{50}\text{Cr}$  was studied in detail by several  $\gamma$ -ray spectroscopy techniques. The measurements were performed at the Munich MP tandem Van de Graaff accelerator with 50–60-cm<sup>3</sup> Ge(Li) detectors of typical

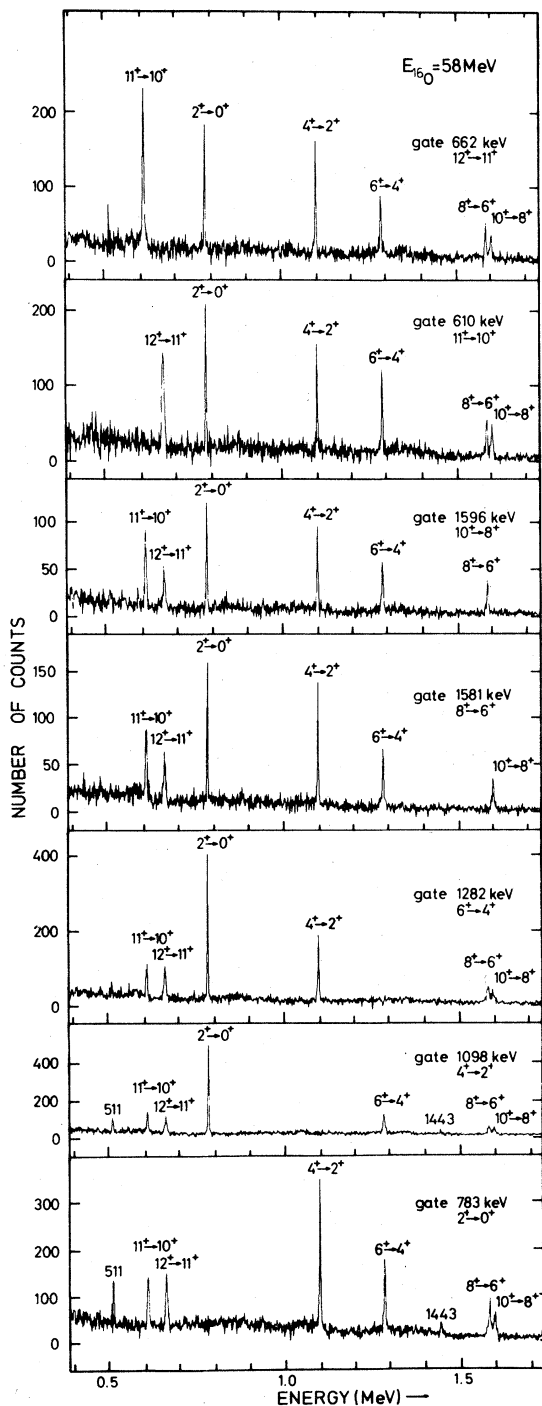


FIG. 1. Results of the  $\gamma$ - $\gamma$  coincidences in the reaction  $^{40}\text{Ca}(^{16}\text{O}, 2p\alpha)^{50}\text{Cr}$ . The  $\gamma$  line at 1443 keV which appears in the 783- and 1098-keV gates originates from the decay of the  $4_2^+$  state in  $^{50}\text{Cr}$  ( $4_2^+ \rightarrow 4_1^+$  transition). The  $4_2^+$  state is mainly populated through the  $\beta^+$  decay of  $^{50}\text{Mn}$  produced via the reaction  $^{40}\text{Ca}(^{16}\text{O}, p\alpha)^{50}\text{Mn}$ .

resolution 2.5 keV (full width at half-maximum) at  $E_\gamma = 332$  keV. All targets consisted of natural metallic calcium. The data acquisition was performed by using the PDP8/PDP10 on-line computer system of this laboratory. The following measurements were performed: (1) excitation functions of  $\gamma$  rays at  $E(^{16}\text{O}) = 37$ –65 MeV; (2)  $\gamma$ - $\gamma$  coincidences with two Ge(Li) detectors at  $90^\circ$  to the beam direction; (3)  $\gamma$ -ray angular distributions between  $0^\circ$  and  $90^\circ$  at seven angles with the Ge(Li) detector 10 cm from the target; (4) Doppler-shift-attenuation lifetime measurements with stopping of ions in Ca (thick target) and Au (thin target) (the thin target consisted of a  $200\text{-}\mu\text{g}/\text{cm}^2$  Ca layer sandwiched between a 0.1-mm-thick Au foil and a  $100\text{-}\mu\text{g}/\text{cm}^2$  Au cover; mean lives have been deduced by a centroid-shift analysis of the  $0^\circ$  and  $90^\circ$  spectra); (5) linear-polarization measurements with a planar Ge(Li) detector according to the method proposed by Ewan *et al.*<sup>8</sup> (the detectors had a shape of  $6 \times 4 \times 0.5$  cm<sup>3</sup> and were positioned at  $90^\circ$  to the beam direction 22.5 cm beneath the target).

In the other reactions mentioned  $\gamma$ - $\gamma$  coincidences and  $\gamma$ -ray excitation functions and angular distributions have been performed. Since they show essentially the same results for the  $^{50}\text{Cr}$  nucleus they will not be presented here.

From several experiments performed with heavy-ion compound reactions it is well accepted<sup>9,12</sup> that mainly the yrast states are populated and the major de-excitation path consists of stretched, downward-cascading  $\gamma$  rays ( $I_f = I_i - I_\gamma$ ,  $I_i > I_f$ ). This can be assumed also in the present case, where a strong selective population of a few  $^{50}\text{Cr}$  levels was observed. (For example, only four levels have been populated in the range  $E_x = 4$ –8 MeV, where more than 60 are known.)

The results from the reaction  $^{40}\text{Ca}(^{16}\text{O}, 2p\alpha)^{50}\text{Cr}$  are summarized in Tables I and II. For the spin and parity assignments the following additional points were considered: (i) States at higher excitation energy and with higher spin have a steeper excitation function than the  $2_1^+$  state. (ii) The relative intensities of the observed  $\gamma$  rays decrease smoothly with increasing excitation energy (Table I). (iii) No crossover transitions exist within a 5% intensity limit. (iv) Nonyrast states like  $4_2^+$  at  $E_x = 3325$  keV are weakly populated (see Fig. 1).

From the comparison of the experimental coefficients  $A_2$  and  $A_4$  (Table I) with the values calculated for total alignment<sup>16</sup> one can assign quadrupole multipolarity to the lowest five transitions

TABLE I. Results of the angular-distribution and linear-polarization measurements in  $^{50}\text{Cr}$ .

Initial		Final		$E_\gamma$ ( $\pm 0.5$ keV)	Rel. $\gamma$ -ray intens. <sup>a</sup> ( $\pm 10\%$ )	Angular distribution				Linear Polarization <sup>c</sup>	
E(keV)	$J^\pi$	E(keV)	J			$A_2$	$A_4$	$\alpha_2^b$	Assign- ment	Predicted P(90°)	Experimental P(90°) <sub>exp.</sub>
782.9	$2^+$	g.s.	$0^+$	782.9	100	$0.22 \pm 0.03$	$-0.03 \pm 0.03$	0.31	E2	$0.35 \pm 0.05$	$0.35 \pm 0.05$
1880.4	$4^+$	782.9	$2^+$	1097.5	97	$0.25 \pm 0.04$	$-0.05 \pm 0.04$	0.49	E2	$0.40 \pm 0.08$	$0.39 \pm 0.07$
3162.4	$6^+$	1880.4	$4^+$	1282.0	85	$0.30 \pm 0.05$	$0.05 \pm 0.07$	0.66	E2	$0.55 \pm 0.10$	$0.48 \pm 0.10$
4743.5	$8^+$	3162.4	$6^+$	1581.1	82	$0.28 \pm 0.06$	$-0.01 \pm 0.07$	0.65	E2	$0.48 \pm 0.13$	$0.59 \pm 0.14$
6339.2	$10^+$	4743.5	$8^+$	1595.7	62	$0.33 \pm 0.11$	$-0.11 \pm 0.14$	0.80	E2	$0.54 \pm 0.26$	$0.53 \pm 0.22$
6949.1	$11^+$	6339.2	$10^+$	609.9	47	$-0.31 \pm 0.03$	$0.01 \pm 0.04$	1.08	M1	$-0.40 \pm 0.05$	$-0.28 \pm 0.07$
		4743.5	$8^+$	(2205.6)	<2						
7610.9	$12^+$	6949.1	$11^+$	661.8	41	$-0.29 \pm 0.04$	$0.05 \pm 0.05$	1.03	M1	$-0.38 \pm 0.05$	$-0.12 \pm 0.10$
		6339.2	$10^+$	(1271.7)	<2						

<sup>a</sup>Measured at  $55^\circ$  to the beam direction. The 783-, 1098-, 1282-, and 662-keV intensities are corrected for the contribution from the  $^{50}\text{Mn}$  activity produced in the reaction  $^{40}\text{Ca}(^{16}\text{O}, p\alpha)^{50}\text{Mn}$ .

<sup>b</sup>The attenuation coefficients are calculated according to Ref. 9.

<sup>c</sup>The definitions of Ref. 13 have been adopted.  $P(90^\circ)_{\text{exp}} = Q^{-1}[(N_\perp - N_\parallel)/\frac{1}{2}(N_\perp + N_\parallel)]$ .  $P(90^\circ)$  is calculated from the measured angular-distribution coefficients under the assumption of  $\delta = 0$ . The quantity  $Q$  is the polarization sensitivity.

and dipole to the 610- and 662-keV lines at the top of the cascade. In addition the spin assignments are supported by the increase of the alignment from the  $J=2$  to the  $J=12$  shown by the coefficients  $\alpha_2$  of Table I.

The sign of  $P(90^\circ)_{\text{exp}}$  (last column of Table I) uniquely determines positive parity for the four new levels ( $8^+$  to  $12^+$ ). The weak polarization of the transition  $12^+ \rightarrow 11^+$  might be due to a small E2 admixture, since a value of  $\delta = 0.05$  is already sufficient to reproduce the measured asymmetry ratio. The lifetime data shown in Table II support some of the parity assignments: Negative parity for the  $J=8, 10$  levels would imply for each one a

$M2$  strength  $> 20$  W.u. (Weiskopf units) and for the  $J=12$  state an E1 strength  $> 0.01$  W.u. which are larger than expected for both cases.

In Fig. 2 the experimental level scheme is compared with the result<sup>17</sup> of a shell-model calculation,<sup>15</sup> in which only  $(1f_{7/2})^n$  configurations are employed. Interesting points in this comparison are the following:

(1) The energy spacings of the middle part of the cascade, namely, for the  $6^+$ ,  $8^+$ , and  $10^+$  states, are extremely well reproduced. However, the inadequacy of only  $(1f_{7/2})^n$  configurations for the whole level sequence is seen in the poor agreement of the lower part of the level scheme,

TABLE II. Electromagnetic transition strengths in  $^{50}\text{Cr}$ .

Transition	$\tau_m$ (psec)	Multi- polarity	$ M ^2$ (W.u.)	
			Experimental	$1f_{7/2}$ theory <sup>b</sup>
$2^+ \rightarrow 0^+$	$12.1 \pm 1.2^a$	E2	$20.4 \pm 2.0$	6.7
$4^+ \rightarrow 2^+$	$3.2 \pm 0.4^a$	E2	$14.3 \pm 1.8$	9.3
$6^+ \rightarrow 4^+$	$1.8 \pm 0.4^a$	E2	$12 \pm 3$	7.6
$8^+ \rightarrow 6^+$	<4	E2	>2	7.1
$10^+ \rightarrow 8^+$	<4	E2	>2	3.4
$11^+ \rightarrow 10^+$	$0.4 < \tau_m < 1.5$	M1	$0.4 > M1 > 0.1$	0.25
$12^+ \rightarrow 11^+$	<0.2	M1	>0.6	1.5

<sup>a</sup>Ref. 4.

<sup>b</sup>Ref. 14; calculation performed with McCullen-Bayman-Zamick wave functions (Ref. 15) and  $e_p = 1.5$ ,  $e_n = 0.5$ ,  $g_p = 1.65$ ,  $g_n = -0.55$ .

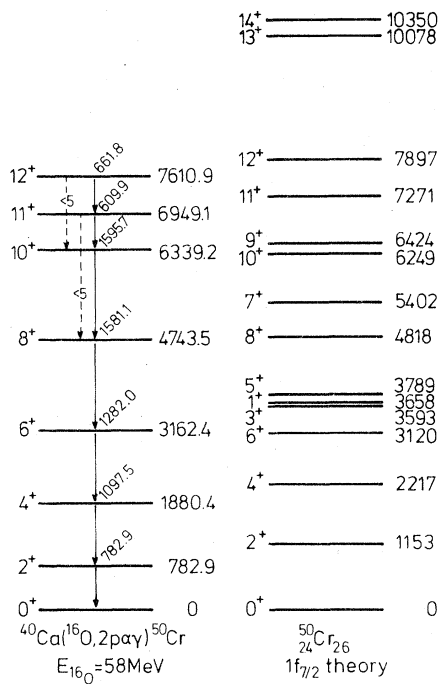


FIG. 2. Decay scheme of  $^{50}\text{Cr}$  observed in the present experiment compared with the results of a shell-model calculation (Ref. 17) with pure  $(1f_{7/2})^n$  configurations.

which should contain more  $2p$  configurations to introduce the necessary collectivity (quasirotational) reflected in the high  $B(E2)$  values of the lowest transitions (Table II).

(2) The appearance of odd-spin states ( $11^+$  in between  $12^+$  and  $10^+$ ) is expected in the shell-model calculation. Such effects are more generally seen in similar calculations, as for example in  $^{212}\text{Po}$ .<sup>18</sup> The nonobservation of lower odd-spin states is reasonable.

(3) The  $M1$  transition probabilities for the transitions  $12^+ \rightarrow 11^+$  and  $11^+ \rightarrow 10^+$  are quite well reproduced by the calculation as shown in Table II.

(4) The  $E2$  transition between the  $12^+$  and  $10^+$  states is not observed (branching ratio  $< 5\%$ ). If one assumes, according to Ref. 14, 1.5 W.u. for the  $M1$  transition from the  $12^+$  to the  $11^+$  state, the  $12^+ \rightarrow 10^+$   $E2$  strength cannot be faster than 15 W.u. This behavior of  $E2$  transitions between the higher members of the band is expected (the calculations<sup>14</sup> predict 4 W.u.).

(5) The situation in  $^{50}\text{Cr}$  resembles in general that for  $^{20}\text{Ne}$ , where extensive experimental and theoretical work has been done. In this nucleus the  $s$ - $d$  shell configurations go only up to  $J^\pi = 8^+$ ,

and the ground-state band has rotationallike energy spacings. However, collective  $E2$  transitions are only observed between lower states while the  $8^+$  one is no more so collective as indicated by experimental data<sup>19</sup> as well as by detailed shell-model calculations.<sup>20</sup>

All the data for the yrast cascade in  $^{50}\text{Cr}$  have similar features to those of  $^{20}\text{Ne}$ , and additionally there is observed the appearance of the  $11^+$  (shell-model) state between the  $12^+$  and  $10^+$  states.

(6) The absence of states above the  $12^+$  may be explained by the results of the calculations, which predict the  $13^+$  and  $14^+$  states to lie far above the  $12^+$  state. From the  $\gamma$ - $\gamma$  coincidences the intensity limit for transitions in the expected energy range was found to be  $\sim 10\%$  compared to that for the transition  $12^+ \rightarrow 11^+$ .

The authors should like to thank Dr. J. Kemmer and Miss H. Hirsch for the fabrication of the Ge(Li) polarimeter.

\*On leave of absence from Istituto di Fisica and Istituto Nazionale di Fisica Nucleare, Padova, Italy.

<sup>1</sup>R. B. Huber, C. Signorini, W. Kutschera, and H. Morinaga, *Nuovo Cimento* **15A**, 501 (1973).

<sup>2</sup>W. Kutschera, R. B. Huber, C. Signorini, and P. Blasi, *Nucl. Phys.* **A210**, 531 (1973).

<sup>3</sup>H. Gögelein *et al.*, in *Proceedings of the International Conference on Nuclear Physics, Munich, Germany, 1973*, edited by J. de Boer and H. J. Mang (North-Holland, Amsterdam, 1973), p. 80.

<sup>4</sup>W. Dehnhardt, O. C. Kistner, W. Kutschera, and H. J. Sann, *Phys. Rev. C* **7**, 1471 (1973).

<sup>5</sup>D. Cline, C. A. Towsley, and R. N. Horoshko, *J. Phys. Soc. Jpn.*, Suppl. **34**, 344 (1973).

<sup>6</sup>K. Nakai, B. Skaali, N. J. Sigurd Hansen, B. Herskind, and Z. Sawa, *Phys. Rev. Lett.* **27**, 155 (1971).

<sup>7</sup>K. Eskola, *Phys. Lett.* **23**, 471 (1966); I. Dervede, *Z. Phys.* **216**, 103 (1968).

<sup>8</sup>G. T. Ewan, G. I. Andersson, G. A. Bartholomew, and A. E. Litherland, *Phys. Lett.* **29B**, 352 (1969).

<sup>9</sup>C. M. Lederer, J. M. Jaklevic, and J. N. Hollander, *Nucl. Phys.* **A169**, 449 (1971).

<sup>10</sup>A. Johnson, H. Ryde, and J. Sztarkier, *Phys. Lett.* **34B**, 605 (1971).

<sup>11</sup>R. M. Lieder *et al.*, *Phys. Lett.* **39B**, 196 (1972).

<sup>12</sup>G. Scharff-Goldhaber, M. McKeown, A. H. Lumpkin, and W. F. Piel, Jr., *Phys. Lett.* **44B**, 416 (1973).

<sup>13</sup>Z. P. Sawa, *Phys. Scr.* **7**, 5 (1973).

<sup>14</sup>B. A. Brown and D. B. Fossan (State University of New York at Stony Brook), private communication.

<sup>15</sup>J. D. McCullen, B. F. Bayman, and L. Zamick, *Phys. Rev.* **134**, B515 (1964).

<sup>16</sup>T. Yamazaki, *Nucl. Data, Sect. A* **3**, 1 (1967).

<sup>17</sup>L. Zamick, private communication; L. Zamick and P. Goode, in *Argonne National Laboratory Informal*

report No. PH-I-1973 B, 1973 (unpublished), p. 697.

<sup>18</sup>N. Auerbach and I. Talmi, Phys. Lett. 10, 297 (1964).

<sup>19</sup>T. K. Alexander, O. Häusser, A. B. McDonald,

A. J. Ferguson, W. T. Diamond, and A. E. Litherland, Nucl. Phys. A179, 477 (1972).

<sup>20</sup>Y. Akiyama, A. Arima, and T. Sebe, Nucl. Phys. A138, 273 (1969).

## Type- $N$ Gravitational Field with Twist

I. Hauser

Physics Department, Illinois Institute of Technology, Chicago, Illinois 60616

(Received 26 August 1974)

I have found a type- $N$  gravitational field for which the principal null direction has non-zero twist and which admits exactly one Killing vector.

In a recent review<sup>1</sup> of the known exact solutions of the Einstein field equations, Kinnersley pointed out that not a single type- $N$  solution with twisting rays<sup>2</sup> was known, though the type- $N$  problem for zero twist had been completely solved<sup>3</sup> over a decade ago. I have now obtained a particular type- $N$  solution with twist. It is my hope that this new solution will further the understanding of gravitational waves with twisting rays. I will now describe the derivation, except for some lengthy techniques which can be extended to the search for other type- $N$  solutions with twist and which will be published elsewhere.

The derivation employs a null tetrad<sup>4</sup> which consists of one-forms  $k$ ,  $m$ ,  $t$ ,  $t^*$  such that  $k$  is a principal null vector,  $k$  and  $m$  are real,  $t^*$  is the complex conjugate of  $t$ , and  $k \cdot m = t \cdot t^* = 1$ . For a type- $N$  vacuum, this null tetrad can be chosen so that the corresponding connection forms have components

$$(\nabla_\alpha k_\beta) t^\beta = \nabla_\alpha \zeta = z(t_\alpha + A k_\alpha), \quad (1)$$

$$(\nabla_\alpha k_\beta) m^\beta = (\nabla_\alpha t_\beta) t^{\beta*} = 0, \quad (2)$$

$$(\nabla_\alpha m_\beta) t^{\beta*} = h \nabla_\alpha \zeta, \quad (3)$$

where  $\zeta$ ,  $z$ ,  $A$ , and  $h$  are complex scalar fields. The real and imaginary parts of  $z$  are the divergence and the twist, respectively. Let

$$z^{-1} = u + i\tau, \quad \sqrt{2}\zeta = \rho + i\sigma, \quad (4)$$

where  $u$ ,  $\tau$ ,  $\rho$ , and  $\sigma$  are real. Then Eqs. (1) and (2) imply that the two-form  $dk$  is given by

$$dk = k(A^* d\zeta + A d\zeta^*) - 2\tau d\rho d\sigma. \quad (5)$$

The particular case for which I have found a solution is defined by the statement that the first term on the right-hand side of Eq. (5) is equal to

$$k(A^* d\zeta + A d\zeta^*) = k d\chi, \quad (6)$$

where

$$d\chi = -d\tau/\tau. \quad (7)$$

Let

$$\Delta = e^{\chi} \tau. \quad (8)$$

Then Eq. (7) is equivalent to the statement that  $\Delta$  is a uniform field, and Eqs. (5) and (6) imply  $d(e^{\chi} k + 2\Delta\rho d\sigma) = 0$ . Hence, there exists a scalar field  $\xi$  such that  $d\xi = e^{\chi} k + 2\Delta\rho d\sigma$ .

$\rho$ ,  $\sigma$ ,  $\xi$ , and  $u$  serve as our coordinates. The solution is given by

$$k = e^{-\chi}(d\xi - 2\Delta\rho d\sigma), \quad (9)$$

$$m = du + 3i\tau(A^* d\zeta - A d\zeta^*), \quad (10)$$

$$t = z^{-1} d\zeta - Ak, \quad (11)$$

$$\tau = \Delta e^{-\chi} = \Delta\rho^{3/2} f(y), \quad y = \xi/\Delta\rho^2, \quad (12)$$

$$A = \sqrt{2}\rho^{-1}[(y-i)f^{-1}f' - \frac{3}{4}], \quad (13)$$

$$h = (3i\Delta/4)(\xi - i\Delta\rho^2)^{-1}, \quad (14)$$

where  $f$  is a function of  $y$ ,  $f' = df/dy$ , such that

$$f'' + \left[\frac{3}{16}(1+y^2)\right]f = 0. \quad (15)$$

The only nonzero components of the Riemann tensor are given by

$$m^\alpha t^{\beta*} m^\gamma t^{\delta*} R_{\alpha\beta\gamma\delta} = 4ze^{\chi} \partial h / \partial \xi. \quad (16)$$

Since none of the scalar coefficients in Eqs. (9) to (11) depends on  $\sigma$ , the tangent vector  $\partial/\partial\sigma$  is a Killing vector.

Any even solution of Eq. (15) has zeros only at  $y = \pm 5.5$ , as determined by a numerical integration; any odd solution has only the one zero at  $y = 0$ . The asymptotic form of any solution of Eq. (15) at large  $y$  is a constant times  $y^{3/4}$  or  $y^{1/4}$ .